

Supplement of Atmos. Chem. Phys., 19, 11865–11886, 2019
<https://doi.org/10.5194/acp-19-11865-2019-supplement>
© Author(s) 2019. This work is distributed under
the Creative Commons Attribution 4.0 License.



Supplement of

Assessment of regional aerosol radiative effects under the SWAAMI campaign – Part 1: Quality-enhanced estimation of columnar aerosol extinction and absorption over the Indian subcontinent

Harshavardhana Sunil Pathak et al.

Correspondence to: Harshavardhana Sunil Pathak (rhsp19@gmail.com)

The copyright of individual parts of the supplement might differ from the CC BY 4.0 License.

In the present document, the details about the network of ground-based observatories (ARFINET and AERONET), the direct measurements from which are used in the present study, are provided in Table S1, S2 and S3 from section S1. The details regarding the estimation of background error covariance matrix, which is required to combine ground-based Absorption AOD (AAOD) with OMI AAOD using 3D-VAR, are illustrated in section S2.

5 S1 ARFINET and AERONET observatories

The present study utilizes the monthly mean AOD data at 500 nm, measured at 27 ARFINET and 17 AERONET stations which are detailed in the Table S1 and S2, respectively. The list of 34 ARFINET observatories, the Black Carbon mass concentration measurements from which are employed in the present study, is provided in Table S3.

Table S1. ARFINET observatories, the AODs from which have been used in the present study.

Sr no.	Station name	Station ID	Latitude in degree north	Longitude in degree east	Altitude in m	Starting year
1	Anantapur (rural, semiarid)	ATP	14.46	77.67	0350	2001
2	Bhubaneswar (semi-urban)	BBR	20.20	85.80	0078	2009
3	Bangalore (urban)	BLR	12.97	77.59	0960	2003
4	Chennai (urban)	CHN	12.70	79.92	0050	2011
5	Dibrugarh (rural)	DBR	27.30	94.60	0111	2002
6	Dehradun (semi-urban, Himalayan Foothills)	DDN	30.34	78.04	0700	2007
7	Delhi (urban)	DEL	28.60	77.20	0239	2012
8	Goa (semi-urban, coastal)	GOA	15.46	73.83	0070	2007
9	Hyderabad (urban)	HYD	17.75	78.73	0557	2003
10	Hyderabad (suburban)	HDT	17.47	78.58	0557	2007
11	Hanle (rural, pristine, high altitude)	HNL	32.78	78.95	4520	2009
12	Imphal (rural)	IPH	24.75	93.92	0765	2010
13	Jaisalmer (rural, desert)	JSL	26.92	70.95	0225	2010
14	Jodhpur (suburban, arid)	JDR	26.26	72.99	0236	1987 a
15	Kashidhoo (rural, island)	KSD	4.96	73.47	1998-2000	
16	Kullu (rural, high altitude)	KLU	31.90	77.10	1154	2009
17	Minicoy (island)	MCY	08.20	73.00	0002	1995 a
18	Mysore (semi-urban)	MYS	12.30	76.50	0772	1989 a
19	Nagpur (urban)	NGP	21.15	79.15	0300	2008
20	Nainital (rural, Himalayan high altitudes)	NTL	29.20	79.30	1960	2002
21	Port Blair (island)	PBR	11.64	92.71	0060	2002
22	Patiala (semi-urban)	PTL	30.33	76.46	0249	2006
23	Shillong (rural, high latitude)	SHN	25.60	91.91	1033	2008
24	Trivandrum (semi-urban, coastal)	TVM	08.50	77.00	0002	1986
25	Udaipur (semi-urban)	UDP	24.60	73.90	0577	2010
26	Visakhapatnam (semi-urban, coastal)	VSK	17.70	83.10	0020	1988
27	Agartala (rural)	AGR	23.50	91.25	0043	2010

In Table S1, locations with population less than 0.5 million are considered as rural, locations having population in between 0.5 to 2 million are considered as semi-urban while locations with population exceeding 2 million are considered to be urban (Babu et al., 2013). Most of the stations mentioned in Table S1 are operational even today except those marked as 'a' in front of respective starting year.

Table S2. AERONET observatories, the AOD from which have been used in the present study.

Sr no.	Station name	Station ID	Latitude in degree north	Longitude in degree east	Starting-end year
1	Baraily (urban)	BRL	28.39	79.43	2008-2008
2	Bhola (semiurban)	BHL	22.69	90.65	2013-2013
3	Dhaka (Urban)	DHK	23.73	90.39	2012-2014
4	EVK2-CNR (rural, Himalayan high altitude)	GCL	27.95	86.81	2006-2011
5	Gandhi college (semi urban)	GCL	25.87	84.12	2006-2014
6	Hanimadhoo (rural, island)	HNM	6.74	73.17	2004-2013
7	Jaipur (arid, urban)	JPR	26.90	75.80	2009-2014
8	Jomsom	JSM	28.77	83.71	2011-2013
9	Kanpur (urban)	KNP	26.51	80.23	2001-2013
10	Kashidhoo (rural, island)	KSD	4.96	73.47	1998-2000
11	Karachi (urban, coastal)	KRC	24.87	67.03	2006-2013
12	Lahore (urban)	LHR	31.54	74.32	2006-2014
13	Male (semiurban, island)	MLE	4.19	73.53	2001-2002
14	Nainital (rural, Himalayan high altitudes)	NTL	29.39	79.45	1998-2012
15	Nam-Co (mountain lake, Himalayan high altitudes)	NMC	30.77	90.00	2006-2011
16	Pantnagar (urban)	PNR	29.05	79.52	2008-2009
18	Patiala (urban)	PTL	30.32	76.39	2006-2012
19	Pokhara (rural, Himalayan valley)	PKR	28.15	83.97	2010-2013
20	QQMS-CAM (semiurban, Himalayan high altitudes)	QQM	28.36	86.94	2010-2014

Table S3. ARFINET observatories, the BC mass concentrations measurements from which have been used in the present study.

Sr no.	Station name	Station ID	Latitude in degree north	Longitude in degree east	Altitude in m	Starting year
1	Agartala (rural)	AGR	23.50	91.25	0043	2010
2	Ahmedabad (urban)	AMD	23.02	72.57	0053	2008
3	Anantapur (rural, semiarid)	ATP	14.46	77.67	0350	2001
4	Bhubaneswar (semi-urban)	BBR	20.20	85.80	0078	2009
5	Bangalore (urban)	BLR	12.97	77.59	0960	2003
6	Chennai (urban)	CHN	12.70	79.92	0050	2011
7	Dibrugarh (rural)	DBR	27.30	94.60	0111	2002
8	Dehradun (semi-urban, Himalayan Foothills)	DDN	30.34	78.04	0700	2007
9	Delhi (urban)	DEL	28.60	77.20	0239	2012
10	Goa (semi-urban, coastal)	GOA	15.46	73.83	0070	2007
11	Hyderabad (urban)	HYD	17.75	78.73	0557	2003
12	Hyderabad (suburban)	HDT	17.47	78.58	0557	2007
13	Hanle (rural, pristine, high altitude)	HNL	32.78	78.95	4520	2009
14	Imphal (rural)	IPH	24.75	93.92	0765	2010
15	Jaisalmer (rural, desert)	JSL	26.92	70.95	0225	2010
16	Kadappa (semi-urban)	KDP	14.46	78.81	0138	2011
17	Kharagpur (rural)	KGP	22.50	87.50	0028	2004
18	Kullu (rural, high altitude)	KLU	31.90	77.10	1154	2009
19	Minicoy (island)	MCY	08.20	73.00	0002	1995 a
20	Mysore (semi-urban)	MYS	12.30	76.50	0772	1989 a
21	Nagpur (urban)	NGP	21.15	79.15	0300	2008
22	Nainital (rural, Himalayan high altitudes)	NTL	29.20	79.30	1960	2002
23	Naliya (rural, coastal)	NAL	22.23	68.89	0050	2007
24	Ooty (rural, high altitude)	OTY	11.40	76.70	2520	2012
25	Port Blair (island)	PBR	11.64	92.71	0060	2002
26	Patiala (semi-urban)	PTL	30.33	76.46	0249	2006
27	Pune (urban)	PUN	18.54	73.85	0457	2005
28	Rajkot (urban)	RKT	22.3	70.8	0140	2008
29	Ranchi (semi-urban)	RNC	23.23	85.23	0654	2010
30	Shillong (rural, high latitude)	SHN	25.60	91.91	1033	2008
31	Trivandrum (semi-urban, coastal)	TVM	08.50	77.00	0002	1986
32	Udaipur (semi-urban)	UDP	24.60	73.90	0577	2010
33	Varanasi (semi-urban)	VNS	25.3	82.96	0078	2009
34	Visakhapatnam (semi-urban, coastal)	VSK	17.70	83.10	0020	1988

S2 3D-VAR : Construction of observational and background covariance matrices

3D-VAR, one of the widely used data assimilation methods based on least square optimization, expresses the assimilated field in terms of parent datasets and their covariance matrices, as shown in the following equation (Kalnay, 2002; Lewis et al., 2006)

$$[B^{-1} + H^T R^{-1} H] X = [B^{-1} X_b + H^T R^{-1} Z] \quad (1)$$

Here, X and X_b refer to MG AAOD and OMI AAOD vectors, respectively, of size $n \times 1$, where 'n' is the total no of grid points in the spatial domain (n=1120 for the current study). Further from equation 1, Z denotes the vector of GR AAODs, which is of size $m \times 1$ where m is the no. of ground-based observatories data from which is used for merging. The map from the grid space and the observation space is provided by the interpolation matrix referred as H (size $m \times n$) in equation 1. Here, H is constructed through bilinear interpolation of gridded background data to the locations of ground-based observatories encompassed by those grid points. Finally, B (size $n \times n$) and O (size $m \times m$) represent the error covariance matrices for OMI AAODs and GR AAODs respectively.

For the successful implementation of 3D-VAR, appropriate construction of B and R is quite important as these covariance matrices not only decide the spatial patterns in which observations are assimilated with the gridded background data but also provides the weights given to the respective parent datasets during the assimilation. The construction of observation error covariance matrix (R) is already detailed in the main article (section 3.2), however the details regarding estimation of background error covariance matrix (B) are as given below.

S2.1 Constructing background error covariance matrix (B)

In the present work, as the observation error covariance matrix has the diagonal structure, the task of deciding the spatial patterns in which GR AAODs blend with the gridded background data, is performed by the background error covariance matrix only. So, the construction of matrix B is a crucial for the present merged product to be realistic. As such, we have made use of time series of OMI AAOD data (500 nm, monthly mean) from 2005 to 2016, for constructing B.

As a first step to estimate B, the data matrix (D) with it's columns formed by X_b at different time instances (say k = no. of time instances) is constructed and thus matrix D has the size of $n \times k$. The climatology of AAOD at each grid point is constructed by taking mean of each row of the data matrix to get the column vector of size $n \times 1$ which we refer as C . The anomaly matrix (referred as A , size $n \times k$) is then constructed as shown in equation 2

$$A(i, j) = D(i, j) - C(i, 1) \quad (2)$$

In equation 2, the index i refers to spatial location and j refers to the time instance. The background error covariance matrix, B is then estimated as shown in equation 3.

$$B = \frac{I}{k-1} A A^T \quad (3)$$

In the above equation 3, I refers to an identity matrix of size $n \times n$.

5 In the view of the statistically estimated matrix B to be realistic, one would opt to employ the longest possible time series of OMI AAOD, which translates to making use of OMI AAODs for all the months during year 2005 to 2016 to construct B . However in that case, the temporal variations (especially at seasonal scale) in OMI AAOD, can lead to bias in the estimated covariance. It is to be noted here that the seasonal variations in AAOD can primarily be associated with seasonal changes in the sources and loading of absorbing aerosol species as well as the meteorological parameters (boundary layer height, large
10 scale wind patterns) over the Indian region.

In order to avoid this potential bias in the estimate of matrix B , we have estimated the background error covariance matrix separately for pre-monsoon season, Mar-Apr-May (MAM) (deeper PBLH causing enhanced vertical mixing of aerosols) and for post-monsoon + winter (Oct to Feb, ONDJF) (shallower PBL and relatively lesser vertical mixing of aerosols). Henceforth, we refer background covariance matrices for pre-monsoon and post monsoon + winter season as B_{PM} and B_{WT} respectively.

15 It is to be noted that, the existence of long-term trend in OMI AAOD is also examined and de-trending is performed if a trend is found significant at 95% confidence level. These de-trended AAODs are then employed for the estimation of B_{PM} and B_{WT} , in order to avoid the bias emanating from probable long-term trend in OMI AAODs. However, due to quite limited length of background data available (36 months for MAM and 60 months for ONDJF during year 2005 to 2016), B_{PM} and B_{WT} are rank-deficient and hence singular. So, in order to make them full rank matrices, we have added a small value ($\sim 10^{-8}$) to the
20 diagonal elements of B_{PM} and B_{WT} , which is known as the method of regularization (Lewis et al., 2006). This addition to the diagonal elements of B_{PM} and B_{WT} is neither altering the structure of covariance matrices nor making significant changes to variances (i.e. diagonal elements) which are of the order of 10^{-6} , for the present study. The regularized B_{PM} and B_{WT} are then employed to respectively estimate the merged AAODs (using equation 1) for the months March to May and October to February.

S3 Subregions of Indian region

Indian domain has been divided into four subregions based on large-scale geographical features, which are detailed in Table 1 from the main manuscript. Those subregions are depicted in the following figure.

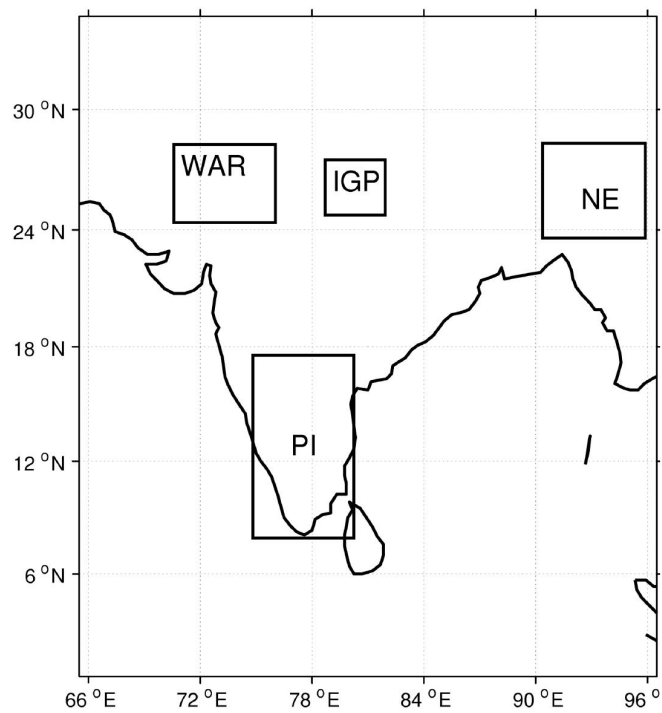


Figure S1. Subregions of the spatial domain

References

- Babu, S. S., Manoj, M. R., Moorthy, K. K., Gogoi, M. M., Nair, V. S., Kompalli, S. K., Satheesh, S. K., Niranjan, K., Ramagopal, K., Bhuyan, P. K., and Singh, D.: Trends in aerosol optical depth over Indian region: Potential causes and impact indicators, *Journal of Geophysical Research: Atmospheres*, 118, 11,794–11,806, <https://doi.org/10.1002/2013JD020507>, <https://agupubs.onlinelibrary.wiley.com/doi/abs/10.1002/2013JD020507>, 2013.
- 5 Kalnay, E.: *Atmospheric Modeling, Data Assimilation and Predictability*, Cambridge University Press, <https://doi.org/10.1017/CBO9780511802270>, 2002.
- Lewis, J. M., Lakshmivarahan, S., and Dhall, S.: *Dynamic Data Assimilation: A Least Squares Approach*, *Encyclopedia of Mathematics and its Applications*, Cambridge University Press, <https://doi.org/10.1017/CBO9780511526480>, 2006.